nature climate change

SUPPLEMENTARY INFORMATION

https://doi.org/10.1038/s41558-018-0227-5

In the format provided by the authors and unedited.

Recent poleward shift of tropical cyclone formation linked to Hadley cell expansion

S. Sharmila[1,2]* and K. J. E. Walsh[1]

[1]School of Earth Sciences, University of Melbourne, Parkville, Australia. [2]Faculty of Science and Technology, Federation University, Mount Helen, Australia. *e-mail: sharmila.climate@gmail.com

Recent poleward shift of tropical cyclone formation linked to Hadley cell expansion

S. Sharmila[*,1,2], K. J. E. Walsh[1]

[1]School of Earth Sciences, University of Melbourne, Australia

[2]Faculty of Science and Technology, Federation University, Australia

SUPPLEMENTARY INFORMATION

Supplementary Table 1:

Suppl. Table ST1: List of CMIP5 models selected for this study along with modelling groups and resolutions.

Model	Modelling Group	Atmospheric Resolution
ACCESS1.0	Commonwealth Scientific and Industrial Research Organization (CSIRO) and Bureau of Meteorology, (BOM), Australia	$1.25^0 \times 1.875^0$ L38
ACCESS1.3	Commonwealth Scientific and Industrial Research Organization (CSIRO) and Bureau of Meteorology, (BOM), Australia	$1.25^0 \times 1.875^0$ L38
BCC-CSM1.1	Beijing Climate Centre, China Meteorological Administration, China	T42L26
BNU-ESM	College of Global Change and Earth System Science, Beijing Normal University, China	T42L26
CanESM2	Canadian Centre for Climate Modeling and Analysis, Canada	T63L35
CCSM4	National Center for Atmospheric Research, USA	$0.9^0 \times 1.25^0$
CESM1-CAM5	National Center for Atmospheric Research, USA	$0.9^0 \times 1.25^0$
GFDL-CM3	Geophysical Fluid Dynamics Laboratory, USA	$2^0 \times 2.5^0$ L48
GFDL-ESM2M	Geophysical Fluid Dynamics Laboratory, USA	$2^0 \times 2.5^0$ L24
HadGEM2-ES	Met Office Hadley Centre, UK	$1.25^0 \times 1.875^0$ L38
INMCM4	Institute for Numerical Mathematics, Russia	$1.5^0 \times 2.0^0$ L21
IPSL-CM5A-LR	Institut Pierre-Simon Laplace, France	$1.875^0 \times 3.75^0$ L39
MIROC-ESM	Japan Agency for Marine-Earth Science and Technology, Atmosphere and Ocean Research Institute (The University of Tokyo), and National Institute for Environmental Studies, Japan	T42L80
MPI-ESM-LR	Max Planck Institute for Meteorology (MPI-M), Germany	T63L47
MRI-CGCM3	Meteorological Research Institute, Japan	T159L48

Supplementary Figures

Supplementary Figure 1: Global map of ocean basins selected for this study.

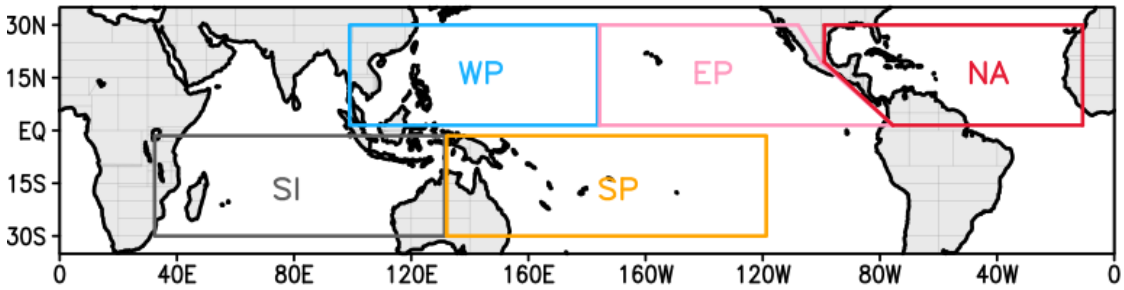

The tropical domains (within 30°N-30°S) selected of the western Pacific (WP), the eastern Pacific (EP), the north Atlantic (NA), the south Indian (SI), and the southern Pacific (SP) oceans. No land points were considered in the above domains.

Supplementary Figure 2: Time series of ENSO and PDO indices

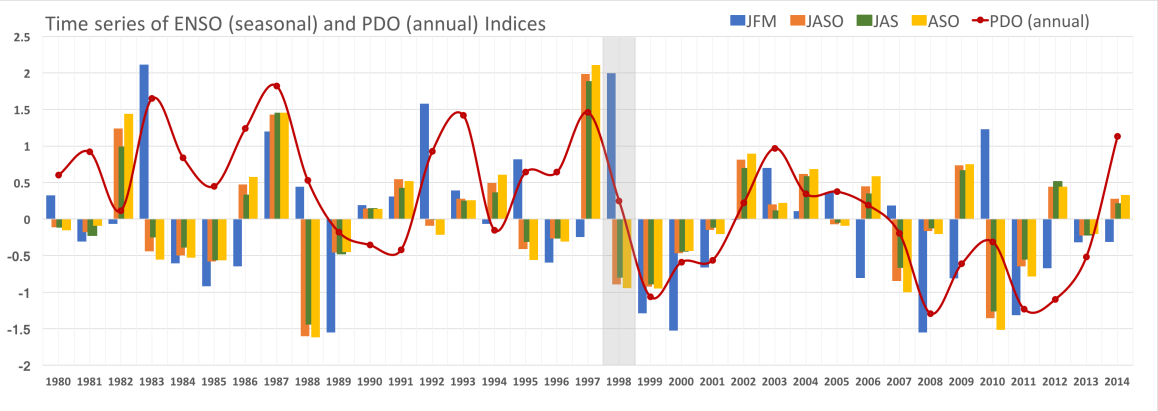

The time series of ENSO (seasonal) and PDO (annual) indices for the study period (1980-2014). Six (nine) moderate-to-strong El Niño/La Niña seasons (when the standard Nino3.4 index was above/below 1°C within the peak season) were identified based on a Nino3.4 index (https://www.esrl.noaa.gov/psd/gcos_wgsp/Timeseries/Nino34/) within 35 peak seasons of individual ocean basins over the northern (southern) hemisphere.

Supplementary Figure 3 | Epochal changes in TCG and large-scale climate conditions as a function of latitude over the five major ocean basins (excluding ENSO effects).

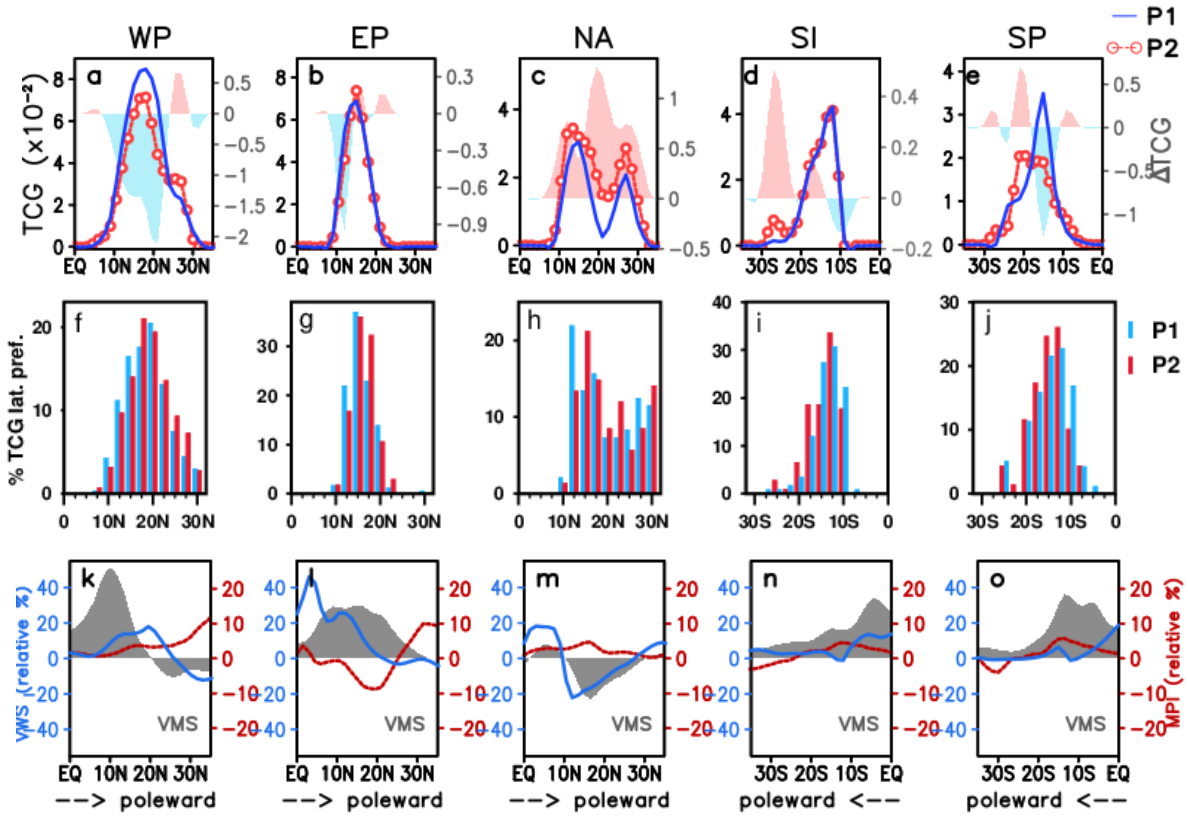

Same as Fig. 2, but excluding the moderate-to-strong ENSO episodes during peak TC seasons of individual ocean basins based on a Nino3.4 index (https://www.esrl.noaa.gov/psd/gcos_wgsp/Timeseries/Nino34/).

Supplementary Figure 4: The relationship between tropical SST anomaly and low-level dry static stability averaged over the deep tropics.

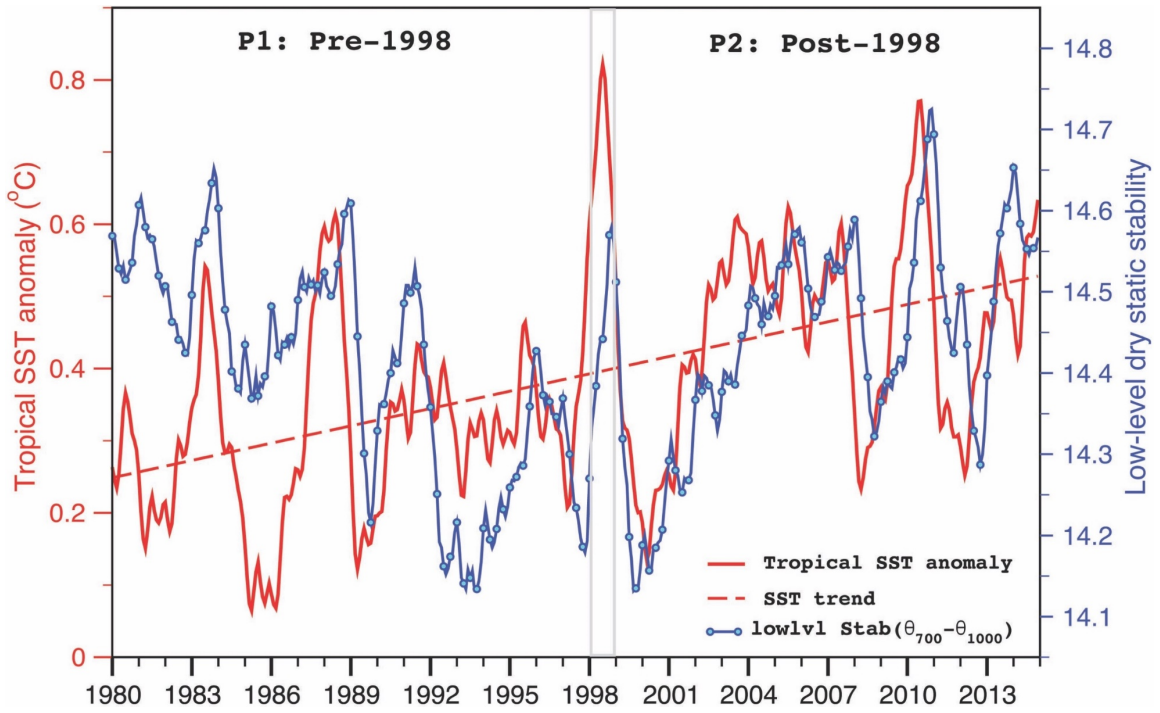

red curve, same as Fig. 1a. **blue curve,** time series of monthly low-level dry static stability (potential temperature difference: $\theta_{700} - \theta_{1000}$) averaged over the deep tropics (10°S-10°N).

Supplementary Figure 5: The relationship between tropical SST anomaly and vertical moisture content averaged over the deep tropics.

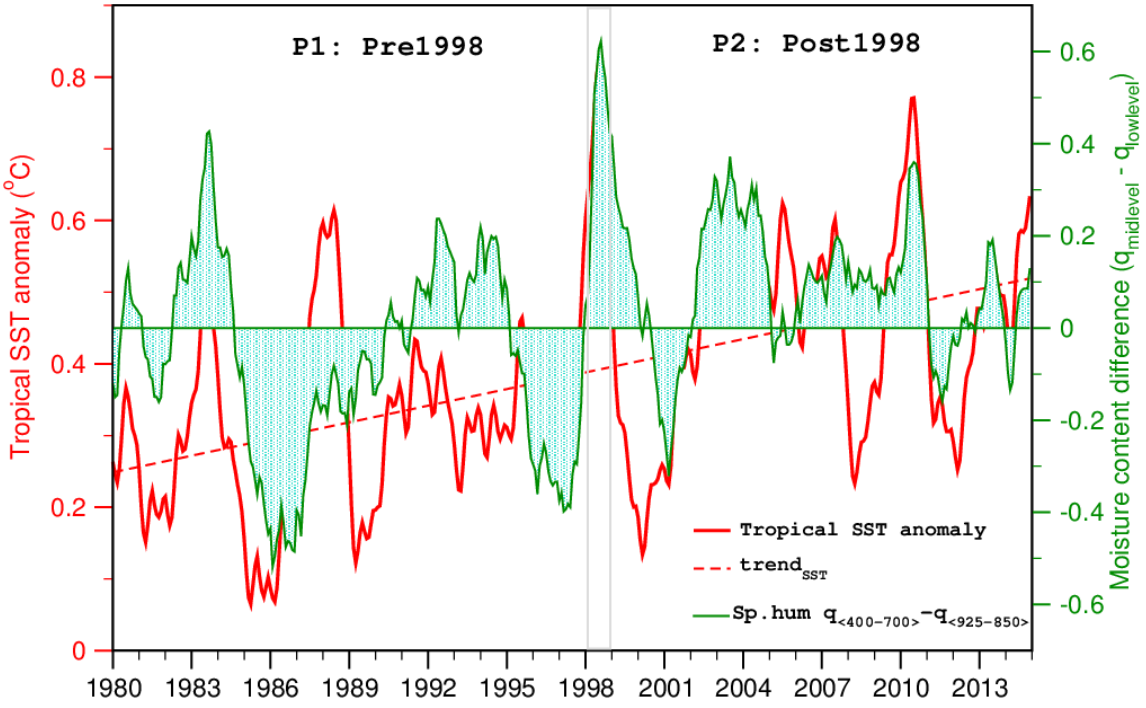

red curve, Same as Fig. 1a. **green curve,** but for the vertical difference in specific humidity between upper <400-700hPa> and lower <925-850hPa> layers of the atmospheric column averaged over the deep tropics (10°S-10°N).

Supplementary Figure 6 | Observed streamfunction (ψ) of the zonal-mean meridional overturning circulation excluding ENSO effect.

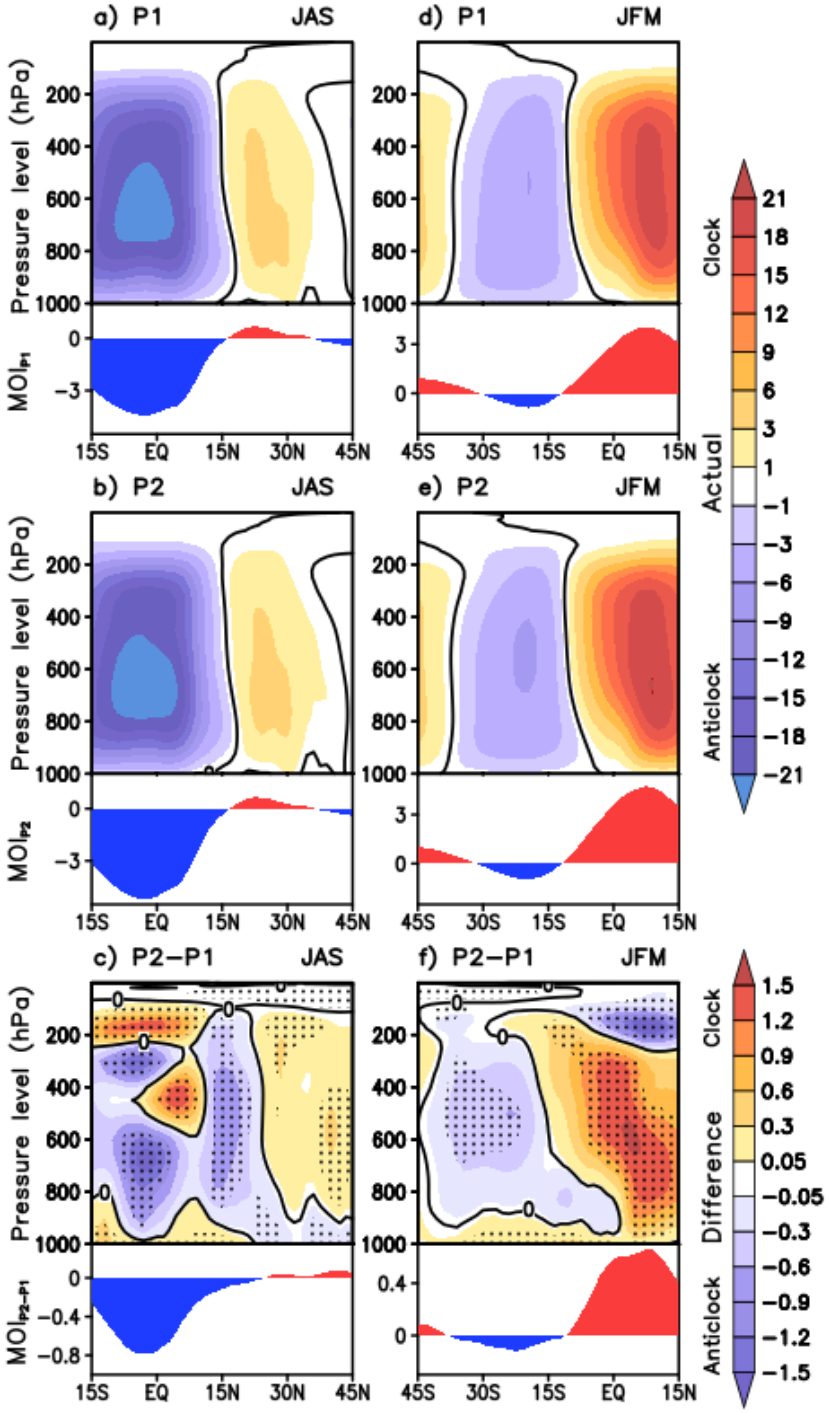

Same as in Fig. 3, but after removing the moderate-to-strong ENSO episodes from the data based on a Nino3.4 index (https://www.esrl.noaa.gov/psd/gcos_wgsp/Timeseries/Nino34/).

Supplementary Figure 7: Multimodel-mean composite of streamfunction (ψ) of the zonal-mean meridional overturning circulation based on CMIP5 models for present climate and projected future changes.

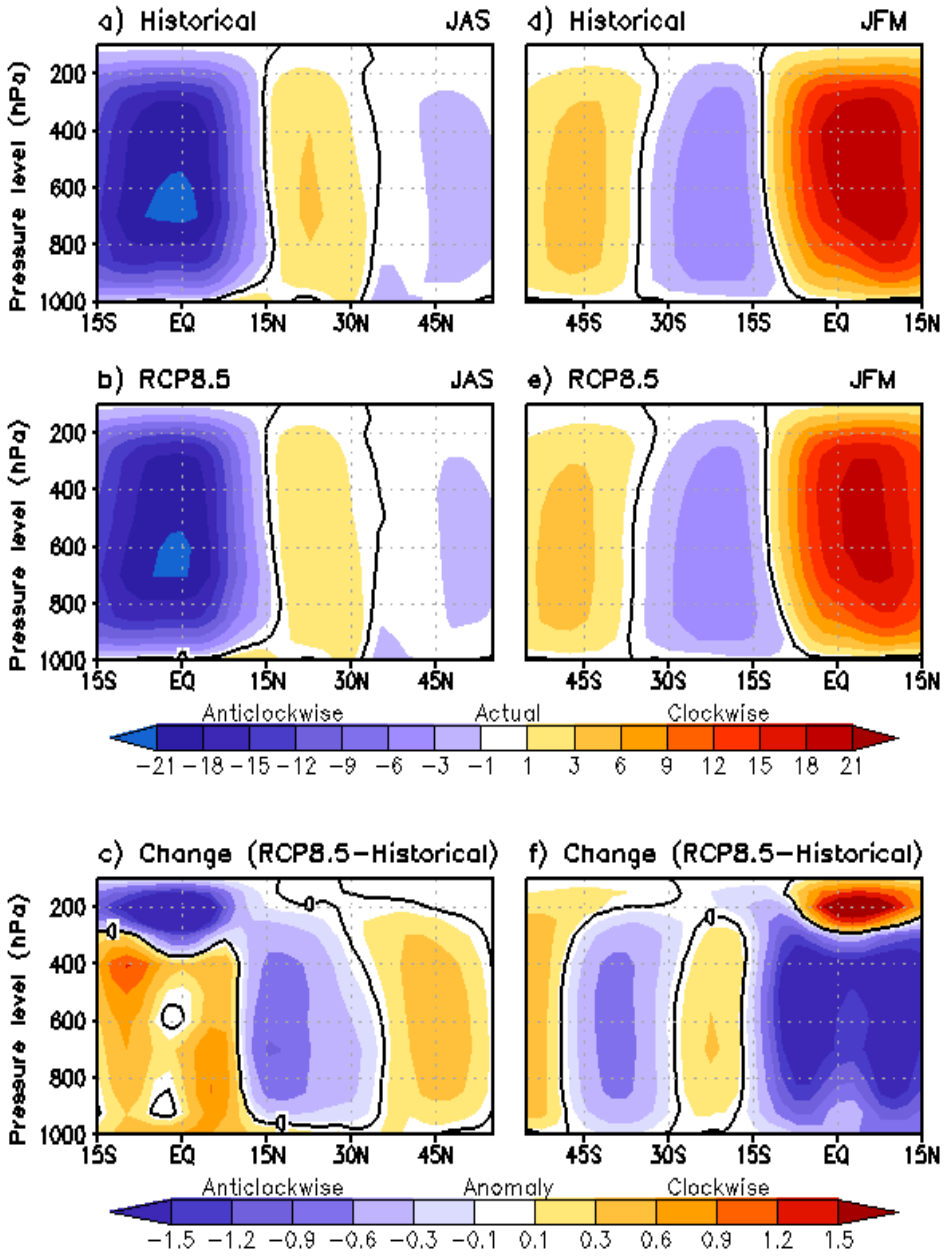

Hadley circulation for present-climate (historical), high-emission scenario (representative concentration pathway 8.5 or RCP8.5: 2160-2095) simulation, and their projected future changes (RCP8.5 - Hist) during (**a-c**), boreal summer (JAS) and (**d-f**), austral summer (JFM). The positive (negative) value of ψ represents clockwise (anti-clockwise) circulation in the latitude-pressure coordinate.

Supplementary Figure 8 | Meridional-vertical structure of the regional Hadley circulation during peak TC seasons over individual basins.

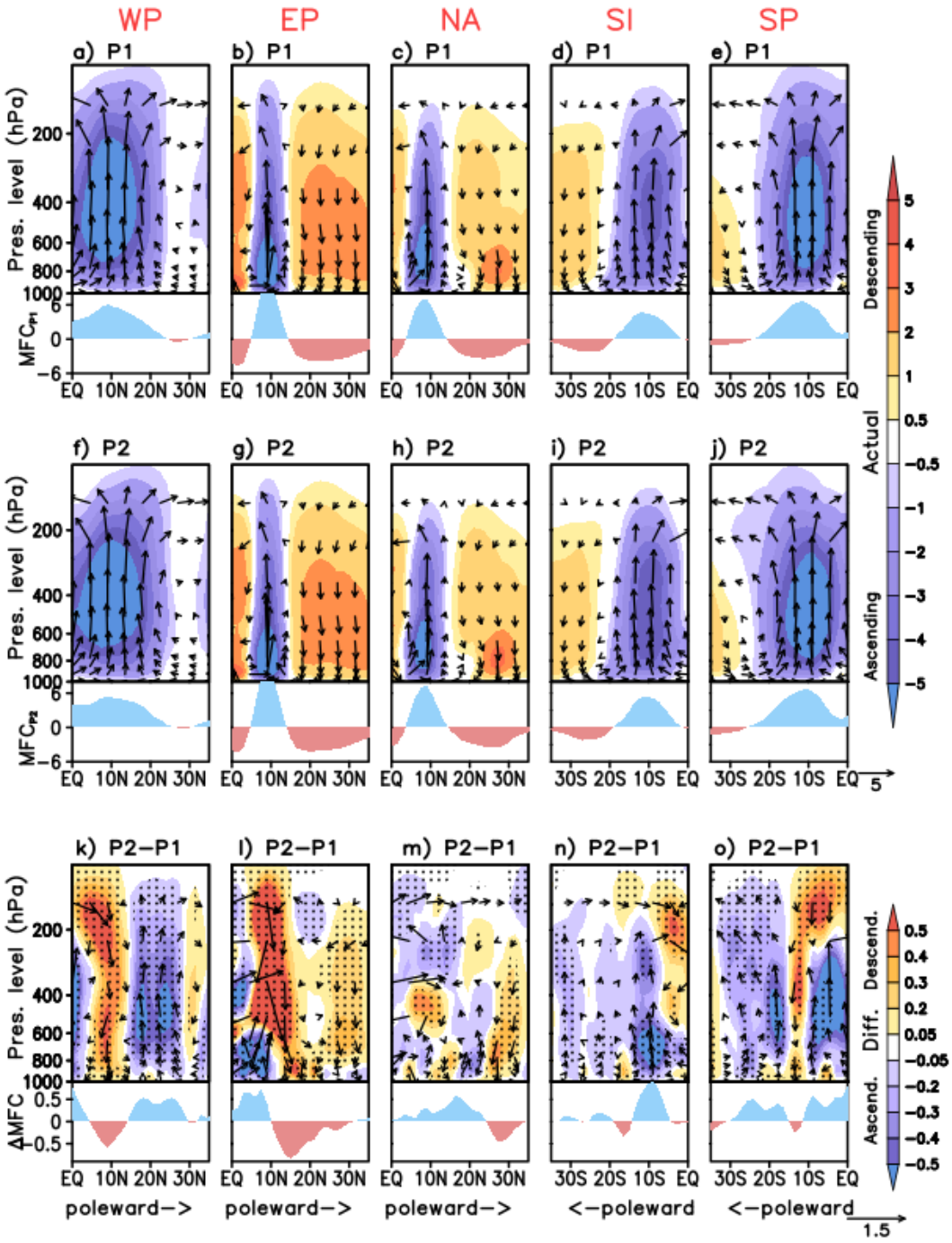

Same as Fig. 4, but excluding the moderate-to-strong ENSO episodes during peak TC seasons of individual ocean basins based on a Nino3.4 index (https://www.esrl.noaa.gov/psd/gcos_wgsp/Timeseries/Nino34/).